Imaging of Misfit Dislocation Formation in Strained Layer Heteroepitaxy by Ultrahigh Vacuum Scanning Tunneling Microscopy

N. Frank, G. Springholz, and G. Bauer
Institut für Halbleiterphysik, Johannes Kepler Universität Linz, A-4040 Linz, Austria
(Received 3 May 1994)

We present a novel technique for the study of strain relaxation in lattice-mismatched heteroepitaxy based on scanning tunneling microscopy. Because of the low limit for detection of single misfit dislocation glide lines, the early stages of strain relaxation can be studied *quantitatively* with high precision. Using this method for the study of molecular beam epitaxy of EuTe on PbTe(111), the existence of an initial sluggish strain relaxation process, undetectable by *in situ* reflection high-energy electron diffraction, is observed in an *actual growth experiment.*

PACS numbers: 68.55.Jk, 61.16.Ch, 61.72.Ff, 68.55.Bd

Strained layer heteroepitaxial growth has attracted considerable interest in the last few years, since it adds more degrees of freedom in the ways to design and fabricate modulated semiconductor heterostructures [1]. The effect of strain on epitaxial growth is of crucial importance, since only for ideal pseudomorphic two-dimensional (2D) layer-by-layer growth sufficiently defect-free layers and morphologically and compositionally sharp interfaces can be obtained. In general, for wetting overlayers on substrates that are not lattice matched, the strains in the layers can be fully accommodated by a biaxial elastic deformation until a critical layer thickness is reached. Beyond this thickness, a network of misfit dislocations is formed at the layer-substrate interface in order to reduce the strain energy in the layer. However, for highly lattice-mismatched systems, the formation of a pronounced surface corrugation (strain-induced coherent islanding [2,3]) has also been found to offer an additional alternative channel for strain relaxation.

In the absence of strain-induced 3D islanding, the usual criterion for the mechanical stability of strained layer structures against formation of misfit dislocations (MD) is given by the Matthews-Blakeslee (MB) "equilibrium" model [4]. In this model, the net force acting on threading dislocations (TD) grown in from the substrate results from the competition between misfit strain force and line tension of the dislocations. When, with increasing layer thickness, the misfit strain force exceeds the line tension, the TD start to move through the layer, creating segments of MD at the layer-substrate interface. Experimentally, the critical layer thicknesses are often found to be larger than predicted by the MB model, especially for low-temperature heteroepitaxial growth [5]. In order to resolve these discrepancies, energetic barriers for propagation, nucleation, and multiplication of dislocations have been included in recent strain relaxation models [6–8], where the key factor for the dislocation dynamics is the "excess stress" in the layers [5]. Thus, three stages in the strain relaxation process are predicted, initially starting rather sluggishly, then accelerating due to increasing excess stress, and finally slowing down when approaching the unstrained bulk state.

As a consequence of the slow initial strain relaxation rate, experimentally, the actual onset of strain relaxation at h_c is not always easily detected. In fact, it has been shown that the experimentally obtained h_c values depend significantly on the detection limit of the various experimental methods [9]. Recent work has demonstrated that the local lattice distortions induced by interfacial dislocations can also be observed by scanning tunneling microscopy (STM) [10,11]. In the present Letter, we show that due to its high spatial resolution, the formation of *single* misfit dislocations in lattice-mismatched epitaxial layers can be studied systematically by STM, and, thus, the initial stages of strain relaxation can be studied *quantitatively* in an actual molecular beam epitaxy (MBE) growth experiment.

The heteroepitaxial system under investigation is EuTe on PbTe(111), and its growth is carried out by MBE [12]. Both materials crystallize in the rock salt structure and their lattice mismatch is 2.1% at room temperature. This combination is interesting for the study of dimensionality effects on magnetic interactions in $(EuTe)_n/(PbTe)_m$ superlattices [13]. First, several μm thick, fully relaxed PbTe buffer layers [11] are deposited on cleaved $BaF_2(111)$ substrates. Because of strain-induced coherent islanding, 2D layer-by-layer growth of EuTe on PbTe(111) exists only in a very narrow regime of growth conditions, where islanding is kinetically suppressed [12]. In the present work, we focus on the Eu-stabilized growth conditions where optimum layer-by-layer growth is observed [12], i.e., for Eu and Te_2 flux rates of 0.4 and 1.2 monolayer (ML)/s, respectively, and a substrate temperature of 270 °C.

The strain relaxation process as well as the evolution of the EuTe surface morphology was studied, combining *in situ* reflection high-energy electron diffraction (RHEED) with STM. The techniques yield complementary information about reciprocal and real-space structure of the surface [14]. For our STM investigations, the

 0031-9007/94/73(16)/2236(4)$06.00

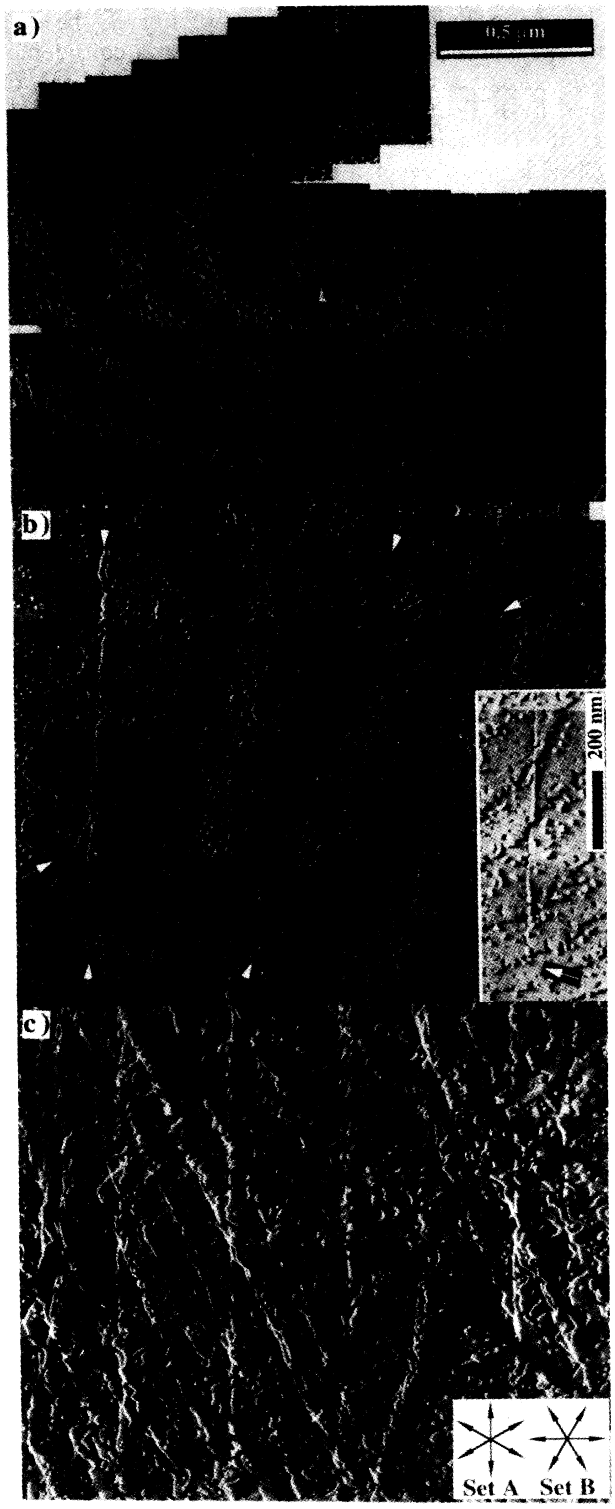

FIG. 1. STM images of EuTe epilayers on PbTe(111) with different layer thicknesses. (a) 20 ML EuTe. The arrow indicates the penetration point of a threading dislocation. (b) 30 ML EuTe. Glide lines are indicated by the arrows. Inset: End point of a MD generated by lateral movement of a TD. (c) 40 ML EuTe. The directions ($\langle \bar{1}10 \rangle$ and $\langle \bar{2}11 \rangle$) of the two sets of glide line are sketched in the lower left corner. The height of the steps is exactly 1 monolayer (1 ML = 3.80 Å).

growth was stopped after well-defined growth sequences, and the samples were rapidly cooled to room temperature. STM experiments are carried out in an attached ultrahigh vacuum (UHV) chamber equipped with a Beetle STM [15]. Large-scale surface maps were mounted together from 20 to 60 single 0.5×0.5 μm^2 STM images. All STM images presented below are unprocessed raw data, which show the local derivative of the height in the horizontal direction.

The surface of the initial PbTe buffer layers is extremely smooth. STM images show that the typical surface features are growth spirals formed around the core of TD (density of the order of 10^7 cm^{-2}) [15] that originate from the 3D nucleation of PbTe on the $BaF_2(111)$ substrates. The curved spiral step edges are all exactly 1 ML in height (3.73 Å), and the step edges are very smooth. The totally flat terraces between the steps have widths of the order of 1000 Å and no 2D islands are nucleated on top of the flat plateaus. For EuTe growth on the PbTe(111) surfaces, initially a very well-defined 2D layer-by-layer growth occurs, giving rise to pronounced RHEED intensity oscillations [12,15]. As a consequence, up to a coverage of about 25 ML, the typical spiraled surface structure of the PbTe buffer is replicated on the EuTe surface. This is shown in Figs. 1(a) and 1(b), where the STM surface images at 20 and 30 ML coverage are depicted.

Although the overall large-scale surface structure of the buffers is replicated by the EuTe layer-by-layer growth on a much more *local* length scale, the EuTe layer surface is much more corrugated. This is a consequence of the much shorter surface diffusion lengths of the adatoms in EuTe MBE growth [15], which results in nucleation of small monolayer islands on the initially flat terraces and in the formation of ragged step edges along the growth spirals (see Fig. 1). At a layer thickness of 25 ML, additional, totally *straight* monolayer surface step lines appear in the large-scale STM images [arrows in Fig. 1(b)], which cut right through all other surface features and displace them by exactly 1 ML in height. Initially, the areal density of these straight lines increases only gradually with the EuTe coverage [see Fig. 1(b)], however, the areal density drastically increases by 1 order of magnitude beyond 35 ML [Fig. 1(c)]. By extensive STM mapping of these surfaces, the end points of these straight lines are identified as penetration points of TD on the surface, as is shown in the inset of Fig. 1(b). Apparently, these have moved by more than 20 μm along the layer surface and, consequently, are clear signatures of MD segments formed at the layer-buffer interface upon strain relaxation by the classical MB mechanism.

In the rock salt crystal structure, the shortest Burgers vector b is of $\frac{1}{2}\langle 110 \rangle$ type and includes an angle of 54.7° with the (111) surface. As is illustrated in Fig. 2, it can be separated into two parts: (1) a component $b_{\parallel}$ parallel to the (111) plane, which relieves in-plane strain, and (2) a perpendicular component $b_{\perp}$, which creates a monolayer

step on the surface along the trace of the moving TD. If the glide took place only in the (100) [011] glide system [Fig. 2(a)], which is typical for the lead salt compounds like PbTe, only three equivalent $\langle \bar{1}10 \rangle$ glide line directions should appear on the (111) surface. Since in the STM images, the glide line directions enclose angles of only 30° [see Fig. 1(c)], a *second* glide system with sixfold symmetry has to be involved in the strain relaxation process. For the rock salt crystal structure, indeed, such a second glide system is well known, namely the $(0\bar{1}1)$ [011] system with $\langle \bar{2}11 \rangle$ glide line directions, typical for the more ionic compounds like NaCl [16]. However, this glide *does not* relieve any misfit strain since, in this particular configuration, the $b_{\parallel}$ component is parallel to the MD line. As a consequence, a different dislocation configuration has to be considered as origin for the $\langle \bar{2}11 \rangle$ glide lines observed on the surface. Such an alternative glide system is shown in Fig. 2(b), where the original TD glides in the $(\bar{3}\bar{1}1)$ plane, yielding an *edge* component $b_{\parallel \mathrm{edge}}$ in the (111) plane, which is essential for misfit strain relief, and a $b_{\perp}$ component, which creates a surface step along the $\langle \bar{2}11 \rangle$ directions. For a number of different glide systems with low index MD line directions, the equilibrium MB critical layer thickness was calculated, using anisotropic linear elasticity theory to compute the self-energy per unit length of the dislocations following the method described in Ref. [16]. Surprisingly, the MB h_c values are nearly identical for the (100) [011] and the alternative $(\bar{3}\bar{1}1)$ [011] glide system (h_c = 14.2 and 16.4 ML, respectively). Considering the uncertainty in the elastic constants of EuTe, which are not known for the actual growth temperature, we conclude that the $(\bar{3}\bar{1}1)$ [011] system is likely to contribute to the strain relaxation process.

With the knowledge of the MD configuration and the magnitude of the in-plane component of the Burgers vector $b_{\parallel \mathrm{edge}}$, the relieved misfit strain $\varepsilon_{\mathrm{rel}}$ can be calculated directly from the areal density ρ of MD lines in the STM images. The such obtained $\varepsilon_{\mathrm{rel}}$ values are plotted in Fig. 3 as a function of the EuTe layer thickness, together with the data from our RHEED measurements [12]. As is indicated in the inset of Fig. 3, the STM data show an onset of strain relaxation at a considerably *smaller* h_c of about 20 ML, as compared to 44 ML obtained by RHEED. Because of the high vertical resolution of STM, surface features of 1 ML in height can easily be identified even in the large scale 2.5 × 2.5 μm^2 images. Thus, considering a regular array of MD with an average spacing of $\leq$2.5 μm between neighboring MD, at least *one* single glide line has to appear in the STM image. For this *areal* density of misfit dislocations (MD length per unit are) of $\rho = 4.0 \times 10^3$ cm^{-1}, the relaxed misfit strain is only $\varepsilon_{\mathrm{rel}} = 10^{-4}$, which is the detection limit for our STM, depending only on the maximum size of the STM images obtained in our experiments. This is more than *10 times* better than the instrumental resolution of 1.5×10^{-3} of RHEED [12]. Although, by transmission electron microscopy, lower MD densities can be detected, it is emphasized that UHV-STM can be used as a *nondestructive,* quasi *in situ* probe for MD. Since the sample surface is preserved, epitaxial growth can be continued after the STM imaging, and, therefore, a whole set of data can be obtained with one single sample. Recently, low-energy electron microscopy (LEEM) has been demonstrated as a new powerful high-resolution *in situ* technique for the imaging of defects and misfit dislocations [17]. However, LEEM is not easily compatible with standard MBE systems and to our knowledge has not been applied for the study of strain relaxation in semiconductors.

Starting at about 20 ML layer thickness, the strain relaxation of EuTe on PbTe(111) proceeds in an extremely *sluggish* manner. Beyond 40 ML, however, the strain relaxation rate drastically increases. It is clear that this behavior can only be explained by considering the kinetics of misfit dislocation multiplication, propagation, and interaction in the strain relaxation process, as was initially proposed by Dodson and Tsao [6] and later refined by several other authors [5,7,8]. For a fit of our strain relaxation data, we use a TD multi-

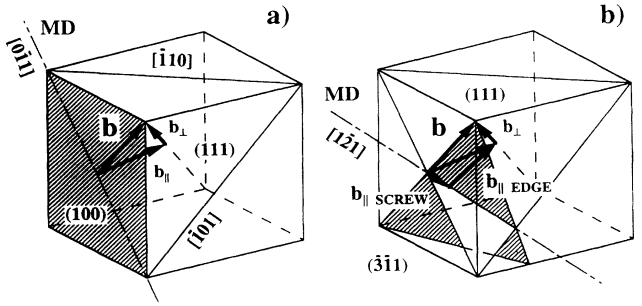

FIG. 2. Schematic illustration of two glide systems in the rock salt crystal structure. (a) (001) [110] and (b) $(\bar{3}\bar{1}1)$ [110]. Dashed-dotted line represents misfit dislocation lines, hatched areas the glide planes.

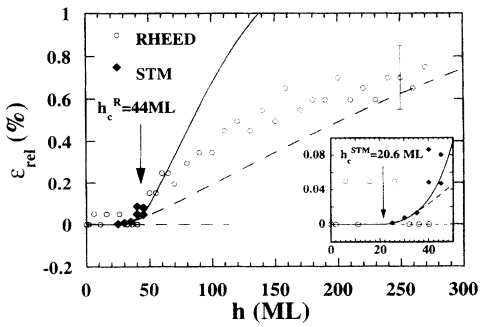

FIG. 3. Relieved misfit strain as a function of the EuTe layer thickness. Diamonds: STM data. Circles: RHEED data. Broken line: calculated fit without dislocation multiplication. Full line: with dislocation multiplication. The inset shows the first stages of strain relaxation on an expanded scale.

plication factor along the lines of Nix *et al.* [7], since in contrast to Si/SiGe, the initial threading dislocation density is already as high as $10^7\ \mathrm{cm}^{-2}$ in the EuTe case. In addition, a frictional force corresponding to the Peierls energy is also taken into account, in agreement with the suggestions of Fox and Jesser [8]. Thus, the essential parameters in the fit of our strain relaxation data are (1) the dislocation velocity, which is assumed to depend linearly on excess stress [6], (2) the dislocation multiplication factor, and (3) the frictional force. It is emphasized that the main goal of our fitting was to reproduce *both* the initial sluggish strain relaxation between 20 and 40 ML, as well as the subsequent acceleration of the strain relaxation rate.

As shown in Fig. 3, the experimental data were fitted (i) with (full line) and (ii) without (dashed line) TD multiplication. Below 40 ML, these two fits do not differ significantly, whereas the strong acceleration in the strain relaxation rate beyond 40 ML can be reproduced *only* by including dislocation multiplication. In spite of this good agreement, the experimental strain relaxation rate decreases appreciably above 70 ML, where the average spacing between neighboring misfit dislocations is already equal to the *total* EuTe layer thickness. As a consequence, interaction between MD, which leads to an increase in their self-energy, can no longer be neglected [5], and, therefore, the actual strain relaxation lags behind the theoretical curve.

From the fit of the STM data, a critical layer thickness of $h_c = 20.5$ ML is obtained, which is still considerably larger than the value of 14.2 ML, according to MB. The difference between the two values indicates a *metastable* pseudomorphic growth regime between the equilibrium MB h_c and the actual onset of strain relaxation at 20.5 ML. This interpretation is verified by post-growth annealing experiments, in which we find a considerable increase of the MD density after the heat treatment. Besides the increase of the number of glide steps on the surface, the surface morphology of the EuTe layers drastically changes beyond a layer thickness of 40 ML. Up to 30 ML, the growth spirals originating from the PbTe buffer layer are still clearly visible, but at larger EuTe thicknesses this feature gradually vanishes, and the surface morphology is dominated by the increasing density of step lines due to TD glide [see Fig. 1(c)], which yields additional sites for the incorporation of the impinged surface adatoms. Further EuTe deposition leads to a distinct waviness of the growth front [15], so that single dislocation glide lines can no longer clearly be resolved. Consequently, STM has to be complemented by a second method, such as RHEED, in order to monitor the whole strain relaxation process.

In conclusion, we have demonstrated that STM provides valuable information not only about the epitaxial atomic scale growth processes [15], but also on the strain relaxation process through misfit dislocations in lattice-mismatched heteroepitaxy. The ability of STM to detect single misfit dislocation glide lines results in a low detection limit of $\epsilon_{\mathrm{rel}} = 1 \times 10^{-4}$ for misfit strain relaxation, and thus the evolution of strain relaxation can be studied *quantitatively*. Using this novel method for the study of lattice-mismatched heteroepitaxial growth of EuTe on PbTe (111), the existence of an initial sluggish strain relaxation process, undetectable by RHEED, is observed in a *real* MBE growth experiment. Because of the sluggish onset of strain relaxation and the much better detection limit, the critical layer thickness determined by STM is almost half of that obtained by RHEED. In addition, it is found that 20 ML beyond the observation of the first misfit dislocation, a drastic increase of the strain relaxation rate occurs, which also leads to a considerable roughening of the surface. The fit of our experiment data reveals that three stages can be distinguished in the observed strain relaxation process: the first stage being dominated by low excess stress, the second stage by dislocation multiplication, and the third stage by interaction between closely spaced dislocations. The precise strain relaxation data obtained by combining UHV-STM with *in situ* RHEED open new possibilities to test the various models for the initial stages of strain relaxation based on different kinds of dislocation nucleation and propagation mechanisms.

This work was supported by the FWF, No. 8446 PHY.

[1] See, e.g., *Semiconductors and Semimetals,* edited by T. P. Pearsall (Academic Press, Boston, 1991), Vol. 33.
[2] C. W. Snyder *et al.,* Phys. Rev. Lett. **66**, 3032 (1991).
[3] D. J. Eaglesham and M. Cerullo, Phys. Rev. Lett. **64**, 1943 (1990).
[4] J. W. Matthews and A. E. Blakeslee, J. Cryst. Growth **27**, 118 (1974); **32**, 265 (1976).
[5] R. Hull and J. C. Bean, Crit. Rev. Solid State Mater. Sci. **17**, 507 (1992).
[6] B. W. Dodson and J. Y. Tsao, Appl. Phys. Lett. **51**, 1325 (1987).
[7] W. D. Nix *et al.,* Mat. Res. Soc. Symp. Proc. **188** (1990).
[8] B. A. Fox and W. A. Jesser, J. Appl. Phys. **68**, 2801 (1990).
[9] I. J. Fritz, Appl. Phys. Lett. **51**, 1080 (1987).
[10] R. Stalder *et al.,* Ultramicroscopy **42–44**, 781 (1992).
[11] G. Meyer, B. Voigtländer, and N. M. Amer, Surf. Sci. **274**, L541 (1992).
[12] G. Springholz and G. Bauer, Phys. Rev. B **48**, 10998 (1993).
[13] J. J. Chen *et al.,* Solid State Electron. **37**, 1073 (1994).
[14] See, e.g., M. G. Lagally, Phys. Today **46**, 24 (1993).
[15] G. Springholz, N. Frank, and G. Bauer, Appl. Phys. Lett. **64**, 2970 (1994).
[16] J. P. Hirth and J. Lothe, *Theory of Dislocations* (Wiley, New York, 1982).
[17] R. M. Tromp *et al.,* Phys. Rev. Lett. **71**, 3299 (1993).

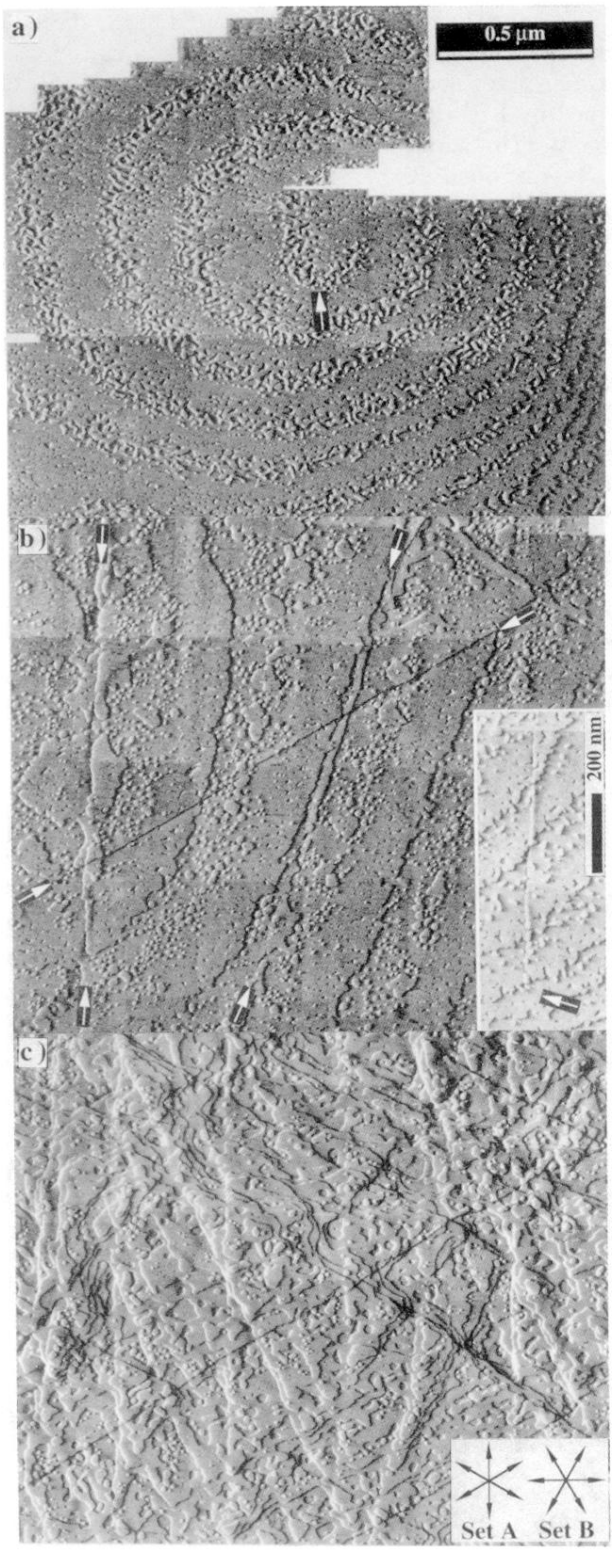

FIG. 1. STM images of EuTe epilayers on PbTe(111) with different layer thicknesses. (a) 20 ML EuTe. The arrow indicates the penetration point of a threading dislocation. (b) 30 ML EuTe. Glide lines are indicated by the arrows. Inset: End point of a MD generated by lateral movement of a TD. (c) 40 ML EuTe. The directions ($\langle \bar{1}10 \rangle$ and $\langle \bar{2}11 \rangle$) of the two sets of glide line are sketched in the lower left corner. The height of the steps is exactly 1 monolayer (1 ML = 3.80 Å).